# Comparison of differential evolution, particle swarm optimization, quantum-behaved particle swarm optimization, and quantum evolutionary algorithm for preparation of quantum states

Xin Cheng(程鑫)[1,†], Xiu-Juan Lu(鲁秀娟)[2,†], Ya-Nan Liu(刘亚楠)[3], and Sen Kuang(匡森)[1,‡]

[1] *Department of Automation, University of Science and Technology of China, Hefei* 230027, *China*
[2] *Department of Mechanical Engineering, The University of Hong Kong, Hong Kong* 999077, *China*
[3] *Quantum Machines Unit, Okinawa Institute of Science and Technology Graduate University, Okinawa* 904-0495, *Japan*

(Received 7 February 2022; revised manuscript received 8 April 2022; accepted manuscript online 11 April 2022)

Four intelligent optimization algorithms are compared by searching for control pulses to achieve the preparation of target quantum states for closed and open quantum systems, which include differential evolution (DE), particle swarm optimization (PSO), quantum-behaved particle swarm optimization (QPSO), and quantum evolutionary algorithm (QEA). We compare their control performance and point out their differences. By sampling and learning for uncertain quantum systems, the robustness of control pulses found by these four algorithms is also demonstrated and compared. The resulting research shows that the QPSO nearly outperforms the other three algorithms for all the performance criteria considered. This conclusion provides an important reference for solving complex quantum control problems by optimization algorithms and makes the QPSO be a powerful optimization tool.

**Keywords:** quantum control, state preparation, intelligent optimization algorithm

**PACS:** 02.60.Pn, 03.65.Aa, 02.30.Yy, 02.60.Cb **DOI:** 10.1088/1674-1056/ac65ee

## 1. Introduction

One goal of quantum control is to guide the dynamics of a quantum system to a desired quantum state or achieve some specific operations,[1,2] which plays an important role in many quantum applications, for example, NMR,[3,4] femtosecond laser,[5] superconducting qubits,[6] and the preparation of quantum gates in quantum computing.[7] Scientists and engineers have developed a variety of methods for the preparation of quantum states, e.g., optimal control,[1] adiabatic control,[8] feedback control,[9] robust control,[10] learning control,[11] and Lyapunov control.[12] Among these methods, learning control has strong application prospects for complex quantum control problems and has been successfully applied to many practical control problems.[6,13–15] In general, learning control can be divided into two categories: gradient-based and gradient-free. The well-known GRAPE and Krotov algorithms belong to gradient-based learning algorithms, which were widely used in numerical simulations and actual experiments.[3,16,17] However, for some complex control problems, it is difficult to obtain the gradient information of a system. In addition, some systems may have local optimal points.[18] In this case, the gradient algorithm is difficult to achieve the control objective. A natural idea to solve such problems is to use random search methods to find optimal control laws. This corresponds to another type of learning methods, i.e., gradient-free intelligent optimization algorithms, including genetic algorithm (GA),[19] particle swarm optimization (PSO),[20] differential evolution (DE),[21] etc. At present, intelligent optimization algorithms have been widely used in quantum physics. For example, GA had been successfully implemented in the control of molecular systems.[11] DE was used for identifying the unknown parameters for different chaotic systems.[22] Dong *et al.*[13,14] proposed an improved DE algorithm to solve the robust quantum control problem. In Refs. [6,15], a direction averaged DE and a subspace-selective self-adaptive DE had been used to find the control pulses for high-fidelity quantum gates respectively. Reference [23] used the PSO combining with the path planning method to determine the unknown parameters in the control laws and realized the high-fidelity transfer to target eigenstates of high-dimensional quantum systems.

Existing studies have shown that PSO and DE have significant advantages over other traditional intelligent optimization algorithms.[24] Based on quantum mechanisms, quantum versions of intelligent optimization algorithms have been developed, e.g., quantum evolutionary algorithm (QEA)[25] and quantum-behaved particle swarm optimization (QPSO).[26] The QEA is a probabilistic optimization method based on quantum computing. It uses qubit encoding to represent chromosomes and quantum-gate updates to complete evolutionary search. The QPSO was invented by incorporating the particle behavior in quantum mechanics and the traditional PSO algorithm. For some problems in other areas, QEA and QPSO

[†]These authors contributed equally.
[‡]Corresponding author. E-mail: skuang@ustc.edu.cn

© 2023 Chinese Physical Society and IOP Publishing Ltd 

are superior to GA and PSO.[27,28] However, they are rarely used in the field of quantum control. Although Zahedinejad *et al.*[29] compared the gradient algorithms and the intelligent optimization algorithms for the preparation of high-fidelity quantum gates, they only considered the traditional DE and PSO. A natural question occurs, that is, do quantum versions of intelligent optimization algorithms perform better with respect to their traditional versions for quantum control problems? In this paper, we will answer this problem and try to provide a valuable reference for the choice of intelligent optimization algorithms solving actual quantum control problems in the future.

In this paper, we use four intelligent optimization algorithms, i.e., DE, PSO, QPSO, and QEA, to find control pulses to achieve the state preparation of closed and open quantum systems. The contributions of this paper are as follows. First, the control performance of the four algorithms is compared and their differences are analyzed. Second, we consider and compare the robustness of the control pulses found by the four algorithms for the perturbed quantum systems. Third, by comparison, a new conclusion is obtained: the QPSO has best performance among the four intelligent optimization algorithms and is almost optimal for all considered performance criteria. This provides an important reference for the future use of intelligent optimization algorithms in solving complex quantum control problems, i.e., the QPSO based on quantum mechanisms is a powerful candidate.

The rest of this paper is organized as follows. Section 2 describes the general closed and open quantum control problems. Section 3 presents the rules of numerical simulation. Numerical simulation results under both undisturbed and disturbed conditions are provided in Section 4. Concluding remarks are given in Section 5.

## 2. Control problem description

In quantum control, one usually decomposes the Hamiltonian of a system into a controllable and an uncontrollable parts and steers the dynamics towards a desired evolution through varying the controllable part.[29]

### 2.1. Closed quantum systems

A quantum system that has no or negligible interactions with the external environment is called a closed quantum system. And for a general $N$-dimensional closed quantum system, its state evolution obeys the following Schrödinger equation:

$$\mathrm{i}\hbar|\dot{\Psi}(t)\rangle = H(t)|\Psi(t)\rangle, \tag{1}$$

where $\mathrm{i}=\sqrt{-1}$, $H(t)=H_0+\sum_{j=1}^{M}u_jH_j$, $H_0$ is the free Hamiltonian of the system, $H_j$ is the $j$th control Hamiltonian, $u_j$ is the $j$th control field, $|\Psi\rangle$ represents the state of the system, and $\hbar$ is the reduced Planck constant (in this paper, we set it as $\hbar=1$).

For the $N$-dimensional closed system in Eq. (1), the quantum state preparation problem can be stated as follows. Within a given time $T$, find suitable controls $u_j$ $(j=1,2,\ldots,M)$ to drive the system to a desired target state $|\Psi_{\mathrm{f}}\rangle$ from a given initial state $|\Psi_0\rangle$ with the highest fidelity possible. To this end, we define fidelity as

$$F := J(u) = |\langle\Psi(T)|\Psi_{\mathrm{f}}\rangle|^2, \tag{2}$$

where $|\Psi(T)\rangle$ is the state of the system at time $T$. Thus, the problem of preparing the target state $|\Psi_{\mathrm{f}}\rangle$ can be expressed as an optimization problem, that is,

$$\max_{u} J(u), \tag{3}$$

s.t.
$$\begin{cases} \mathrm{i}\hbar|\dot{\Psi}(t)\rangle = (H_0+\sum_{j=1}^{M}u_jH_j)|\Psi(t)\rangle, \\ |\Psi(0)\rangle = |\Psi_0\rangle, \quad t\in[0,T]. \end{cases}$$

### 2.2. Open quantum systems

A quantum system that has non-negligible interactions with the external environment is called an open quantum system. Its dynamic evolution is no longer consistent with the unitary evolution, because the interaction with the external environment causes decoherence. Therefore, the state of the system cannot be described by the state vector $|\Psi\rangle$ in Eq. (1), but by the density matrix $\rho$. The $N$-dimensional open quantum system's dynamic evolution can be described by the Lindblad master equation as[30]

$$\dot{\rho} = -\frac{\mathrm{i}}{\hbar}[H(t),\rho(t)] + \sum_{k}\gamma_k\mathfrak{D}[L_k]\rho(t), \tag{4}$$

where the non-negative coefficients $\gamma_k$ specify the relevant relaxation rates of the $k$th channel (in this paper, we set it as $\gamma_k$ =1), $L_k$ are appropriate Lindblad operators, and

$$\mathfrak{D}[L_k]\rho = L_k\rho L_k^{\dagger} - \frac{1}{2}L_k^{\dagger}L_k\rho - \frac{1}{2}\rho L_k^{\dagger}L_k. \tag{5}$$

The first term on the right side of the equal sign of Eq. (4) represents the Schrödinger term, and the second term is the dissipation term, which represents the decoherence effect caused by the interaction between the system and the environment. When the dissipation term is 0, Eq. (4) can be regarded as the dynamic evolution equation of the closed quantum system, which is equivalent to Eq. (1). The derivation from the evolution equation (1) of the closed system to the evolution equation (4) of the open quantum system is referred to Ref. [30].

For the open system (4), we define a coherence vector as $\boldsymbol{x} := (x_1,x_2,x_3,\ldots,x_m)^{\mathrm{T}} = (\mathrm{tr}(U_1\rho),\mathrm{tr}(U_2\rho),\ldots,\mathrm{tr}(U_m\rho))^{\mathrm{T}}$,

where $iU_1, iU_2, \ldots, iU_m$ $(m = N^2-1)$ are a set of orthogonal generators of the special unitary group $SU(N)$. Thus, the density matrix can be written as[31]

$$\rho = \frac{I}{N} + \frac{1}{2}\sum_{l=1}^{m} x_l U_l. \tag{6}$$

By substituting Eq. (6) into Eq. (4), the open quantum system (4) can be expressed as the following coherence vector equation:

$$\dot{\boldsymbol{x}} = (\mathfrak{L}_{H_0} + \mathfrak{L}_{\mathfrak{D}})\boldsymbol{x} + \sum_{j=1}^{M} u_j \mathfrak{L}_{H_j}\boldsymbol{x} + l_0, \tag{7}$$

where the superoperators $\mathfrak{L}_{H_0}$, $\mathfrak{L}_{\mathfrak{D}}$, and $\mathfrak{L}_{H_j}$ $(j = 1,2,\ldots,M)$ are $(N^2-1)\times(N^2-1)$ square matrices, and $l_0$ is an $(N^2-1)$-dimensional column vector. Their specific forms are[31,32]

$$(\mathfrak{L}_{H_0})_{st} = \mathrm{Tr}(iH_0[U_s, U_t]), \tag{8}$$

$$(\mathfrak{L}_{H_j})_{st} = \mathrm{Tr}(iH_j[U_s, U_t]), \tag{9}$$

$$(\mathfrak{L}_D)_{st} = \sum_{j=1}^{N^2-1}\Big(\mathrm{Tr}(L_j^\dagger U_s L_j U_t) - \frac{1}{2}\mathrm{Tr}(L_j^\dagger L_j U_s U_t + L_j^\dagger L_j U_t U_s)\Big), \tag{10}$$

$$(l_0)_s = \frac{1}{N}\sum_{j=1}^{N^2-1}\Big(\mathrm{Tr}([L_j, L_j^\dagger])U_s\Big), \tag{11}$$

where $(\cdot)_{st}$ represents the element of the $s$th row and the $t$th column of a matrix, and $\mathrm{Tr}(\cdot)$ is the trace of a matrix. The fidelity is defined as[32]

$$F := J(u) = 1 - \frac{N}{8(N-1)}||\boldsymbol{x}_{\mathrm{f}} - \boldsymbol{x}(T)||^2, \tag{12}$$

where $||\cdot||$ is a vector norm, $\boldsymbol{x}_{\mathrm{f}}$ is the coherence vector of the target state and $\boldsymbol{x}(T)$ is that of the system state at time $T$. Similarly, the control task can be described as the following optimization problem:

$$\max_{u} J(u), \tag{13}$$

s.t.

$$\begin{cases} \dot{\boldsymbol{x}} = (\mathfrak{L}_{H_0} + \mathfrak{L}_{\mathfrak{D}})\boldsymbol{x} + \sum_{j=1}^{M} u_j \mathfrak{L}_{H_j}\boldsymbol{x} + l_0, \\ \boldsymbol{x}(0) = \boldsymbol{x}_0, \quad t \in [0,T]. \end{cases}$$

## 3. Comparison backgrounds

In this section, we list several backgrounds for the comparison of the four algorithms.

1) **Control fields** We adopt piecewise constant controls for $u_j$ in Eqs. (1) and (4), that is, we discretize the time interval $[0,T]$ into $D$ equal time segments, where the length of each segment is $\delta t = T/D$ and the control $u_j$ takes a constant in each segment. Thus, our control task is to find a suitable pulse sequence $u(1), u(2), u(3), \ldots, u(D)$ on $[0,\delta t)$, $[\delta t, 2\delta t)$, $\ldots$, $[(D-1)\delta t, D\delta t]$ to drive the system to the desired target state. In this paper, we take $T = 4$ a.u. and $D = 100$.

2) **Control amplitudes** In practical applications, the amplitude of $u_j$ is usually bounded, that is, $u_j(k) \in [u_{\min}, u_{\max}]$. In this paper, we assume that $u_{\max} = 10$ and $u_{\min} = -10$.

3) **Hyperparameters** For the parameters in each algorithm, we set their values as follows.

DE: The scaling factor is $F = 0.5$ and the crossover factor is $CR = 0.3$.

PSO: The two learning factors are $c_1 = 1$ and $c_2 = 1$.

QPSO: The contraction-expansion coefficient $\alpha = 0.5$.

QEA: The quantum gate updating rule is provided in Ref. [25].

4) **Evaluation criteria** In this paper, the fidelity will be our performance indicator. The process of intelligent optimization algorithm starts from an initial population and seeks the optimal solution of the optimization problem through continuous iteration. Therefore, in order to ensure fairness in the algorithm evaluation process, we take the following measures: 1) the initial population size of the four algorithms remains the same, which is 100; 2) considering that each algorithm needs to randomly generate initial solutions, we repeat each algorithm 10 times (10 episodes) to reduce the effect of randomness, and the best, mean and worst fidelities of the 10 episodes will be used to measure the performance of the algorithms, where the mean fidelity that best characterizes the actual performance of the algorithms will be prioritized; 3) for each episode, the termination conditions of the four algorithms are also the same, that is, the number of iterations reaches 10000.

5) **Data availability** Please refer to the Appendix for the details of the data of the system models in numerical simulations.

6) **Numerical simulation platform** The computer configuration is intel (R) Core (TM) i9-10900KF CPU @3.7 GHz, RAM 64 GB, Windows 10, MATLAB 9.9.0.1467703 (R2020b).

## 4. Comparison of algorithms

For the problem of quantum state preparation discussed in Section 2, we conduct numerical simulations on two-level, three-level and four-level quantum systems under both undisturbed and disturbed conditions, and at the same time compare the performance of the four algorithms presented in this paper.

### 4.1. Results and analysis

In this section, several closed and open systems are considered in simulations. The simulation results are shown in Table 1 and Fig. 1, where Table 1 presents three types of fidelities (i.e., $F_{\mathrm{best}}$, $F_{\mathrm{mean}}$, and $F_{\mathrm{worst}}$) for the four algorithms and six quantum system models and Fig. 1 describes how the mean fidelity of 10 episodes changes with the iteration number.

**Table 1.** The simulation results of the four algorithms without disturbances, where each algorithm runs 10 episodes with $F_{\text{best}}$, $F_{\text{mean}}$, and $F_{\text{worst}}$ being the best, mean, and worst fidelities of 10 episodes, respectively. The optimal values are in bold and the data greater than 0.99995 are regarded as 1.

| Quantum control problems | DE | | | PSO | | | QPSO | | | QEA | | |
|---|---|---|---|---|---|---|---|---|---|---|---|---|
| | $F_{\text{best}}$ | $F_{\text{mean}}$ | $F_{\text{worst}}$ | $F_{\text{best}}$ | $F_{\text{mean}}$ | $F_{\text{worst}}$ | $F_{\text{best}}$ | $F_{\text{mean}}$ | $F_{\text{worst}}$ | $F_{\text{best}}$ | $F_{\text{mean}}$ | $F_{\text{worst}}$ |
| Two-level closed system | **1.0000** | **1.0000** | **1.0000** | **1.0000** | **1.0000** | **1.0000** | **1.0000** | **1.0000** | **1.0000** | **1.0000** | **1.0000** | **1.0000** |
| Three-level closed system | 0.9999 | 0.9998 | 0.9997 | **1.0000** | **1.0000** | 0.9999 | **1.0000** | **1.0000** | **1.0000** | 0.9997 | 0.9982 | 0.9960 |
| Four-level closed system | 0.9955 | 0.9935 | 0.9902 | 0.9993 | 0.9951 | 0.9855 | **1.0000** | **1.0000** | **1.0000** | 0.9691 | 0.9402 | 0.8941 |
| Two-level open system | 0.9813 | 0.9791 | 0.9776 | 0.9833 | 0.9788 | 0.9754 | **0.9854** | **0.9843** | **0.9826** | 0.9719 | 0.9704 | 0.9688 |
| Three-level open system | 0.9541 | 0.9484 | 0.9412 | 0.9493 | 0.9208 | 0.8872 | **0.9672** | **0.9612** | **0.9560** | 0.9023 | 0.8907 | 0.8772 |
| Four-level open system | 0.9493 | 0.9208 | 0.8980 | 0.9502 | 0.9088 | 0.8805 | **1.0000** | **0.9973** | **0.9899** | 0.8922 | 0.8617 | 0.8420 |

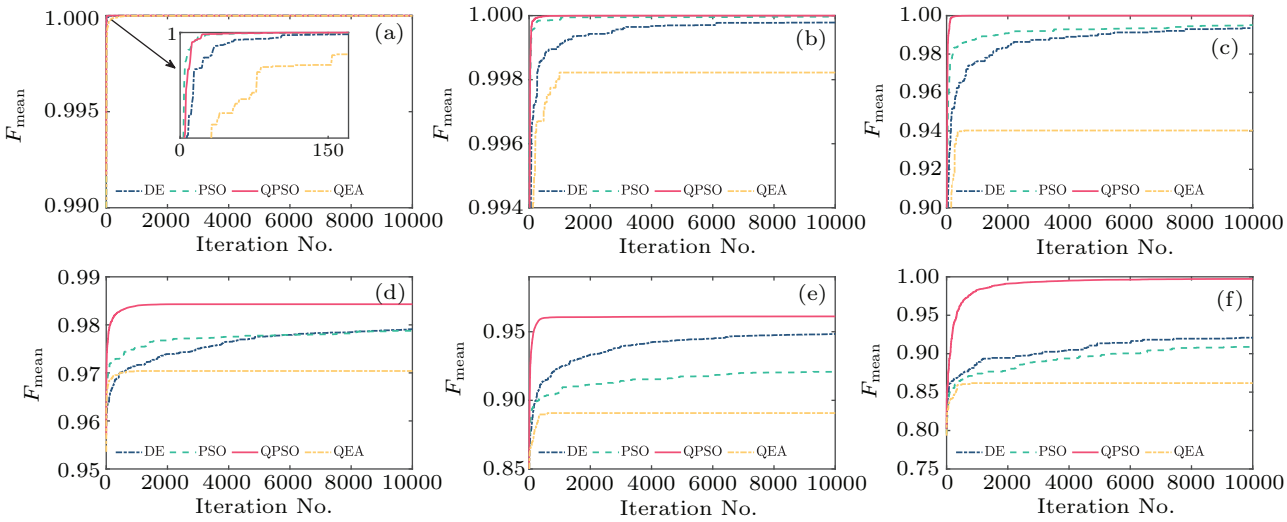



**Fig. 1.** Quantum state preparation of six quantum systems: $F_{\text{mean}}$ vs. iteration No. of the four algorithms. The $F_{\text{mean}}$ here refers to the mean fidelity of the algorithm running 10 episodes. (a) Two-level closed quantum system; (b) three-level closed quantum system; (c) four-level closed quantum system; (d) two-level open quantum system; (e) three-level open quantum system; (f) four-level open quantum system.

From Table 1, we can clearly obtain the following three conclusions. First, for the problem of state preparation of both closed and open quantum systems, QPSO outperforms the other three algorithms in the best, mean and worst fidelities of 10 episodes. And the superior performance of QPSO is more obvious for open quantum systems. For example, the mean fidelity of QPSO under 10 episodes is 0.9973 for the four-level open quantum system, which is 8.3%, 9.7% and 15.7% higher than those of DE, PSO and QEA, respectively. Second, the performance of QEA is worst with respect to the other three algorithms in all the aspects except for the two-level closed system. Third, PSO has a slight advantage over DE for closed quantum systems and it is reversed for open quantum systems.

Figure 1 can also describe the characteristics of the four algorithms in the iterative process. Compared with the other three algorithms, QPSO can always achieve a best performance and converges at a fast rate, while QEA performs worst and stops converging after several iterations for all these six quantum systems.

One might ask why QEA is bad and QPSO is excellent. For the QEA with the quantum gate update mechanism, a quantum gate is used to update the position of each particle. The rotation angle of the quantum gate is determined by a simple look-up table, which leads to the discontinuity of the updated value of each rotation and makes the update insufficient. On the other hand, the QEA is easy to fall into local optimums and therefore performs poorly in the quantum control problem. The superiority of the QPSO algorithm can be explained from its essential features. First, a particle described by a probability density function can appear in any region of the entire feasible search space with a certain probability. This enables each particle not to be restricted by velocity and therefore can converge faster. Second, in the iterative process, the average best position is introduced to assisting in updating the position of each particle, which can avoid all particles moving toward the present optimal value. Thus, the algorithm is not easy to fall into local optimal values, which actually improves the global search ability. Moreover, compared with the other three algorithms, the number of parameters of QPSO is least, which can improve the efficiency of adjusting the algorithm parameters.

According to the simulation results, QPSO is the best while QEA is the worst for the state preparation of closed and open quantum systems without disturbances. This provides us with an important reference when using intelligent optimization algorithms to solve some quantum control problems, i.e., QPSO should be given a high priority.

### 4.2. Robustness

In this section, we consider the robustness of the four algorithms in the presence of disturbances. For an actual quantum system, there are always some external disturbances, inaccurate models, and errors in the control field. Here, we assume that the Hamiltonian of the systems in Eqs. (1) and (4) has the following form:[13]

$$H_{\Theta}(t) = f_0(\theta_0)H_0 + \sum_{m=1}^{M} f_m(\theta_m)u_m(t)H_m\,, \tag{14}$$

where $\Theta = (\theta_0, \theta_1, \ldots, \theta_M)$ and $f_m(\theta_m)$ $(m = 0, 1, 2, \ldots, M)$ describes possible uncertainties. $f_0(\theta_0)$ represents the uncertainty of the free Hamiltonian, e.g., the chemical shift in NMR. $f_m(\theta_m)$ characterizes possible noises in the control fields or imprecise parameters in the dipole approximation. We assume that $f_m(\theta_m)$ are continuous functions of $\theta_m$ and the parameters $\theta_m$ takes values in $[1-E_m, 1+E_m]$, $E_m \in [0,1]$. For simplicity, we also assume that all uncertain boundaries satisfy $E_0 = \cdots = E_m = \cdots = E_M = E = 0.2$ and $\theta_m$ is equal to 1 in the absence of disturbance.

Based on the sampling learning method, we take the two-level open system as an example to compare the robustness of the algorithms. For convenience, we set $f_0(\theta_0) = \theta_0$ and $f_m(\theta_m) = \theta_m$. In the numerical simulation, we choose 9 training samples. Both $\theta_0$ and $\theta_m$ take values of 0.8, 1.0 and 1.2 in turn, thus forming $3 \times 3 = 9$ samples.

We first generate optimal control pulses for the four algorithms under 10 episodes by 9 trained samples as shown in Fig. 2. To compare the robustness of the optimal pulses found by these four algorithms, we randomly selected 100 test samples for testing. Both $\theta_0$ and $\theta_m$ randomly take 10 values in $[0.8, 1.2]$, thus forming $10 \times 10 = 100$ samples. The test results are presented in Fig. 3.

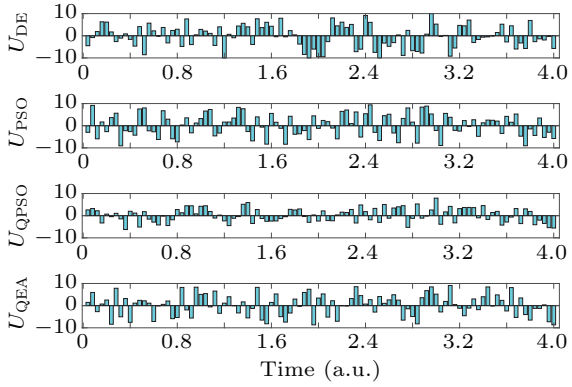



**Fig. 2.** The control pulses of the four algorithms learned by 9 training samples.

From Fig. 3, we can see that QPSO is still a best choice, and the fidelities of all test samples are steady and high with respect to the other three algorithms, which shows that the control pulses trained by QPSO not only have best robustness but also have best control performance. The fidelities of DE in the test samples are more concentrated than those of PSO, that is, the trained control pulses are more robust. QEA still ranks bottom, the minimum fidelity of the test samples is nearly 0.92, lower than 0.98 corresponding to QPSO. And the fidelities of the test samples have large fluctuation range, which implies a poor robustness of control pulses.

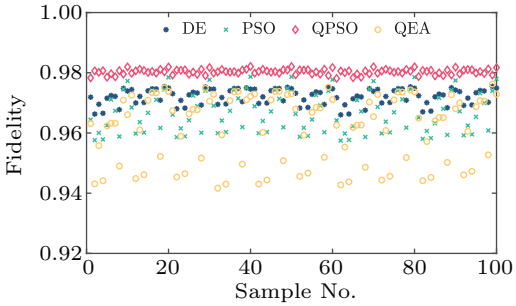



**Fig. 3.** The fidelity of 100 test samples under control pulses in Fig. 2.

Figure 4 shows the effect of the fluctuations of $\theta_0$ and $\theta_m$ on the fidelities associated with the four algorithms. It is easily seen that the fidelity surface under the QEA is steepest in the parameter fluctuation space, which indicates a worst robustness. In contrast, the fidelity surface under QPSO is above those under the other three algorithms. Moreover, the fidelity surface under QPSO is relatively flat, which means that the corresponding control pulses have best robustness.

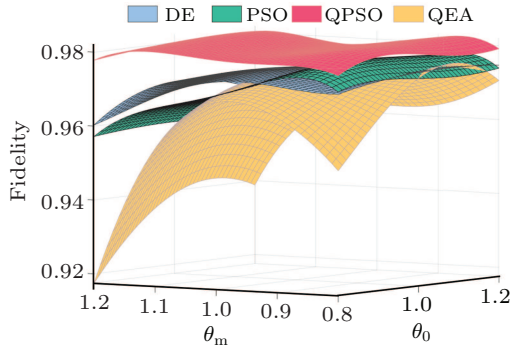



**Fig. 4.** The robustness control landscape defined as the fidelity versus two uncertainty parameters under control pulses in Fig. 2.

## 5. Conclusion

DE and PSO have been widely used in various quantum control problems. However, QPSO and QEA based on quantum mechanisms are rarely used in the field of quantum control. In this article, we used the four intelligent optimization algorithms (DE, PSO, QPSO, and QEA) to find control pulses to achieve the state preparation of closed and open quantum systems. The research in this paper shows that QPSO has best performances and QEA ranks bottom when disturbances are not considered. While for robust control problems with disturbances, QPSO still performs best and has obvious advantages over the other three algorithms. This provides an essential reference for the use of intelligent optimization algorithms solving complex quantum control problems, that is, QPSO is a powerful candidate.

## Appendix A: Data for system models

### Two-level closed quantum system model

The two energy eigenstates of the two-level closed quantum system are $|1\rangle = (1,0)^{\mathrm{T}}$, $|2\rangle = (0,1)^{\mathrm{T}}$. The Hamiltonian is

$$H(t) = H_0 + u(t)H_1,$$

where $H_0 = \begin{pmatrix} 0.5 & 0 \\ 0 & -0.5 \end{pmatrix}$, $H_1 = \begin{pmatrix} 0 & 0.5 \\ 0.5 & 0 \end{pmatrix}$. The initial state and final state can be described as $|\Psi_0\rangle = \frac{1}{\sqrt{2}}(1,1)^{\mathrm{T}}$ and $|\Psi_{\mathrm{f}}\rangle = (0.6, 0.8\mathrm{i})^{\mathrm{T}}$, respectively.

### Three-level closed quantum system model

The three energy eigenstates of the three-level closed quantum system are $|1\rangle = (1,0,0)^{\mathrm{T}}$, $|2\rangle = (0,1,0)^{\mathrm{T}}$, $|3\rangle = (0,0,1)^{\mathrm{T}}$. The Hamiltonian is

$$H(t) = \sum_{j=1}^{3} 0.2j(j-1)|j\rangle\langle j| + u(t)H_1,$$

where

$$H_1 = |1\rangle\langle 2| + |2\rangle\langle 1| + |1\rangle\langle 3| + |3\rangle\langle 1| + |2\rangle\langle 3| + |3\rangle\langle 2|.$$

The initial state and final state can be described as $|\Psi_0\rangle = (1,0,0)^{\mathrm{T}}$ and $|\Psi_{\mathrm{f}}\rangle = (0,1,0)^{\mathrm{T}}$, respectively.

### Four-level closed quantum system model

The four energy eigenstates of the four-level closed quantum system are $|1\rangle = (1,0,0,0)^{\mathrm{T}}$, $|2\rangle = (0,1,0,0)^{\mathrm{T}}$, $|3\rangle = (0,0,1,0)^{\mathrm{T}}$, $|4\rangle = (0,0,0,1)^{\mathrm{T}}$. The Hamiltonian is

$$H(t) = \sum_{j=1}^{4} 0.25j(j+1)|j\rangle\langle j| + u(t)(\sin\varphi H_1 + \cos\varphi H_2),$$

where $\varphi = \frac{1}{6}\pi$,

$$H_1 = |1\rangle\langle 2| + |2\rangle\langle 1| + |2\rangle\langle 3| + |3\rangle\langle 2| + |3\rangle\langle 4| + |4\rangle\langle 3|,$$
$$H_2 = |1\rangle\langle 3| + |3\rangle\langle 1| + |2\rangle\langle 4| + |4\rangle\langle 2| + |1\rangle\langle 4| + |4\rangle\langle 1|.$$

The initial state and final state can be described as $|\Psi_0\rangle = (1,0,0,0)^{\mathrm{T}}$ and $|\Psi_{\mathrm{f}}\rangle = (0,0,1,0)^{\mathrm{T}}$, respectively.

### Two-level open quantum system model

The two energy eigenstates of the two-level open quantum system are $|1\rangle = (1,0)^{\mathrm{T}}$, $|2\rangle = (0,1)^{\mathrm{T}}$. The Hamiltonian is

$$H(t) = H_0 + u(t)H_1.$$

where $H_0 = \begin{pmatrix} 0.5 & 0 \\ 0 & -0.5 \end{pmatrix}$, $H_1 = \begin{pmatrix} 0 & 0.5 \\ 0.5 & 0 \end{pmatrix}$. The Lindblad operator is given the following form:[33]

$$L_1 = 0.2|1\rangle\langle 2|, \quad L_2 = 0.1|2\rangle\langle 1|, \quad L_3 = 0.2|1\rangle\langle 1|.$$

The initial state and final state can be described as $\rho_0 = |1\rangle\langle 1|$ and $\rho_{\mathrm{f}} = |2\rangle\langle 2|$, respectively.

### Three-level open quantum system model

The three energy eigenstates of the three-level open quantum system are $|1\rangle = (1,0,0)^{\mathrm{T}}$, $|2\rangle = (0,1,0)^{\mathrm{T}}$, $|3\rangle = (0,0,1)^{\mathrm{T}}$. The Hamiltonian is

$$H(t) = \sum_{j=1}^{3} 0.2j(j-1)|j\rangle\langle j| + u(t)(\sin\varphi H_1 + \cos\varphi H_2),$$

where $\varphi = \frac{1}{6}\pi$,

$$H_1 = |1\rangle\langle 2| + |2\rangle\langle 1| + |2\rangle\langle 3| + |3\rangle\langle 2|,$$
$$H_2 = |1\rangle\langle 3| + |3\rangle\langle 1|.$$

The Lindblad operator is given the following form:[33]

$$L_1 = 0.4|1\rangle\langle 2|, \quad L_2 = 0.2|1\rangle\langle 3|, \quad L_3 = 0.3|2\rangle\langle 3|.$$

The initial state and final state can be described as $\rho_0 = |1\rangle\langle 1|$ and $\rho_{\mathrm{f}} = |3\rangle\langle 3|$, respectively.

### Four-level open quantum system model

The four energy eigenstates of the four-level open quantum system are $|1\rangle = (1,0,0,0)^{\mathrm{T}}$, $|2\rangle = (0,1,0,0)^{\mathrm{T}}$, $|3\rangle = (0,0,1,0)^{\mathrm{T}}$, $|4\rangle = (0,0,0,1)^{\mathrm{T}}$. The Hamiltonian is

$$H(t) = \sum_{j=1}^{4} 0.25j(j+1)|j\rangle\langle j| + u(t)(\sin\varphi H_1 + \cos\varphi H_2),$$

where $\varphi = \frac{1}{6}\pi$,

$$H_1 = |1\rangle\langle 2| + |2\rangle\langle 1| + |2\rangle\langle 3| + |3\rangle\langle 2| + |3\rangle\langle 4| + |4\rangle\langle 3|,$$
$$H_2 = |1\rangle\langle 3| + |3\rangle\langle 1| + |2\rangle\langle 4| + |4\rangle\langle 2|.$$

The Lindblad operator is given the following form:[33]

$$L_1 = 0.4|1\rangle\langle 2|, \quad L_2 = 0.3|1\rangle\langle 3|,$$
$$L_3 = 0.2|1\rangle\langle 4|, \quad L_4 = 0.3|2\rangle\langle 3|,$$
$$L_5 = 0.2|2\rangle\langle 4|, \quad L_6 = 0.3|3\rangle\langle 4|.$$

The initial state and final state can be described as $\rho_0 = |1\rangle\langle 1|$ and $\rho_{\mathrm{f}} = |3\rangle\langle 3|$, respectively.

## Acknowledgement

Project supported by the National Natural Science Foundation of China (Grant No. 61873251).

## References


[1] Dong D and Petersen I R 2010 *IET Control Theory & Applications* **4** 2651
[2] Brif C, Chakrabarti R and Rabitz H 2010 *New J. Phys.* **12** 075008
[3] Khaneja N, Reiss T, Kehlet C, Schulte-Herbrüggen T and Glaser S J 2005 *Journal of Magnetic Resonance* **172** 296
[4] Lu D, Li K, Li J, Katiyar H, Park A J, Feng G, Xin T, Li H, Long G, Brodutch A, Baugh J, Zeng B and Laflamme R 2017 *npj Quantum Information* **3** 1
[5] Assion A, Baumert T, Bergt M, Brixner T, Kiefer B, Seyfried V, Strehle M and Gerber G 1998 *Science* **282** 919
[6] Zahedinejad E, Ghosh J and Sanders B C 2015 *Phys. Rev. Lett.* **114** 200502
[7] Schulte-Herbrüggen T, Spörl A, Khaneja N and Glaser S 2005 *Phys. Rev. A* **72** 042331
[8] Shapiro E, Milner V, Menzel-Jones C and Shapiro M 2007 *Phys. Rev. Lett.* **99** 033002
[9] Yamamoto N, Tsumura K and Hara S 2007 *Automatica* **43** 981
[10] Lu X J and Kuang S 2019 *IET Control Theory & Applications* **13** 711
[11] Rabitz H, de Vivie-Riedle R, Motzkus M and Kompa K H 2000 *Science* **288** 824
[12] Kuang S and Cong S 2008 *Automatica* **44** 98
[13] Dong D, Xing X, Ma H, Chen C, Liu Z and Rabitz H 2019 *IEEE Transactions on Cybernetics* **50** 3581
[14] Ma H, Dong D, Shu C C, Zhu Z and Chen C 2017 *Control Theory and Technology* **15** 226
[15] Yang X, Li J and Peng X 2019 *Science Bulletin* **64** 1402
[16] Eitan R, Mundt M and Tannor D J 2011 *Phys. Rev. A* **83** 053426
[17] Kuang S, Qi P and Cong S 2018 *Phys. Lett. A* **382** 1858-1863
[18] Rabitz H A, Hsieh M M and Rosenthal C M 2004 *Science* **303** 1998
[19] Holland J H 1992 *Scientific American* **276** 66
[20] Venter G and Sobieszczanski-Sobieski J 2003 *AIAA Journal* **41** 1583
[21] Storn R and Price K 1997 *Journal of Global Optimization* **11** 341
[22] Li N Q, Pan W, Yan L S, Luo B, Xu M F and Jiang N 2011 *Chin. Phys. B* **20** 060502
[23] Guan X, Kuang S, Lu X and Yan J 2020 *IEEE Access* **8** 49765
[24] Vesterstrom J and Thomsen R 2004 *Proceedings of the 2004 Congress on Evolutionary Computation*, June 19–23, 2004, Portland, USA **2** 1980–1987
[25] Han K H and Kim J H 2002 *IEEE Transactions on Evolutionary Computation* **6** 580
[26] Sun J, Fang W, Wu X, Palade V and Xu W 2012 *Evolutionary Computation* **20** 349
[27] Meng K, Wang H G, Dong Z and Wong K P 2009 *IEEE Transactions on Power Systems* **25** 215
[28] Zhang G 2011 *Journal of Heuristics* **17** 303
[29] Zahedinejad E, Schirmer S and Sanders B C 2014 *Phys. Rev. A* **90** 032310
[30] Breuer H P and Petruccione F 2022 *The Theory of Open Quantum Systems* (Oxford: Oxford University Press)
[31] Kimura G 2003 *Phys. Lett. A* **314** 339
[32] Yang F, Cong S, Long R, Ho T S, Wu R and Rabitz H 2013 *Phys. Rev. A* **88** 033420
[33] Lindblad G 1976 *Communications in Mathematical Physics* **48** 119